BK_{Ca} channel regulates calcium oscillations induced by alpha-2-macroglobulin in human myometrial smooth muscle cells

Monali Wakle-Prabagaran[a], Ramón A. Lorca[a], Xiaofeng Ma[a], Susan J. Stamnes[b], Chinwendu Amazu[a], Jordy J. Hsiao[b], Celeste M. Karch[c], Krzysztof L. Hyrc[d], Michael E. Wright[b], and Sarah K. England[a,b,d,1]

[a]Department of Obstetrics and Gynecology, Washington University School of Medicine, St. Louis, MO 63110; [b]Department of Molecular Physiology and Biophysics, University of Iowa, Iowa City, IA 52242; [c]Department of Psychiatry and Hope Center for Neurological Disorders, Washington University School of Medicine, St. Louis, MO 63110; and [d]Center for the Investigation of Membrane Excitability Diseases, Washington University School of Medicine, St. Louis, MO 63110

Edited by Richard W. Aldrich, The University of Texas at Austin, Austin, TX, and approved March 9, 2016 (received for review September 16, 2015)

The large-conductance, voltage-gated, calcium (Ca^{2+})-activated potassium channel (BK_{Ca}) plays an important role in regulating Ca^{2+} signaling and is implicated in the maintenance of uterine quiescence during pregnancy. We used immunopurification and mass spectrometry to identify proteins that interact with BK_{Ca} in myometrium samples from term pregnant (≥37 wk gestation) women. From this screen, we identified alpha-2-macroglobulin (α_2M). We then used immunoprecipitation followed by immunoblot and the proximity ligation assay to confirm the interaction between BK_{Ca} and both α_2M and its receptor, low-density lipoprotein receptor-related protein 1 (LRP1), in cultured primary human myometrial smooth muscle cells (hMSMCs). Single-channel electrophysiological recordings in the cell-attached configuration demonstrated that activated α_2M (α_2M*) increased the open probability of BK_{Ca} in an oscillatory pattern in hMSMCs. Furthermore, α_2M* caused intracellular levels of Ca^{2+} to oscillate in oxytocin-primed hMSMCs. The initiation of oscillations required an interaction between α_2M* and LRP1. By using Ca^{2+}-free medium and inhibitors of various Ca^{2+} signaling pathways, we demonstrated that the oscillations required entry of extracellular Ca^{2+} through store-operated Ca^{2+} channels. Finally, we found that the specific BK_{Ca} blocker paxilline inhibited the oscillations, whereas the channel opener NS11021 increased the rate of these oscillations. These data demonstrate that α_2M* and LRP1 modulate the BK_{Ca} channel in human myometrium and that BK_{Ca} and its immunomodulatory interacting partners regulate Ca^{2+} dynamics in hMSMCs during pregnancy.

BK_{Ca} | α2M | LRP1 | myometrial smooth muscle | intracellular calcium

During pregnancy, the human myometrium remains relatively quiescent until near term, when it becomes more sensitive to contractile stimuli (1). At term, synchronized phasic contractions develop and increase in strength and frequency to facilitate labor. Phasic contractions require the myometrial smooth muscle cells (MSMCs) to alternate between states of contraction and relaxation. The primary trigger for initiating and maintaining spontaneous contractions is an increase in the intracellular level of the major charge carrier calcium (Ca^{2+}) (2–4), which occurs by multiple mechanisms (5, 6), One, Ca^{2+} can enter through voltage-gated channels in response to membrane depolarization. Two, agonist stimulation can cause ligand binding to receptor-operated channels that allow extracellular Ca^{2+} to enter the cell to increase intracellular Ca^{2+} ($[Ca^{2+}]_i$). Three, agonist [e.g., oxytocin (OXT)] can bind to receptors that induce Ca^{2+} release from intracellular stores, including the sarcoplasmic reticulum, by activating signal transduction pathways (2). Lastly, store-operated Ca^{2+} entry (SOCE) can occur in response to sarcoplasmic reticulum store depletion. The rise in $[Ca^{2+}]_i$ activates Ca^{2+}-calmodulin, myosin light chain kinase, and the actomyosin machinery, thus leading to MSMC contraction (2, 7).

MSMC relaxation occurs by several mechanisms. First, myosin light chain kinase and myosin light chain phosphatase are inhibited by phosphorylation and dephosphorylation, respectively (8). Additionally, $[Ca^{2+}]_i$ is reduced by extrusion of Ca^{2+} from the cytosol by plasma membrane Ca^{2+}-ATPases and sequestration of Ca^{2+} into internal stores by sarcoplasmic reticulum Ca^{2+}-ATPases (6). Finally, K^+ efflux through Ca^{2+}-activated K^+ channels repolarizes the MSMC membrane, thereby inducing closure of voltage-dependent Ca^{2+} channels and returning the cell to a resting state and $[Ca^{2+}]_i$ to basal levels (9).

The predominant K^+ channel in the myometrium is the large-conductance, voltage-gated, Ca^{2+}-activated K^+ channel (BK_{Ca}), also known as MaxiK/hSlo/KCa1.1 (10–12). Opening of the BK_{Ca} channel provides a strong repolarizing current to maintain MSMCs at a polarized membrane potential, thus preventing voltage-gated Ca^{2+} influx and contraction. Conversely, pharmacological block of BK_{Ca} channels depolarizes human MSMCs (hMSMCs), causing activation of voltage-sensitive L-type Ca^{2+} channels and increased $[Ca^{2+}]_i$ (13). BK_{Ca} is activated by both depolarization of the plasma membrane and increases in $[Ca^{2+}]_i$ (13). In vascular smooth muscle cells, BK_{Ca} is also activated by Ca^{2+} sparks elicited by activation of ryanodine receptors in the sarcoplasmic reticulum (14), but this mechanism of BK_{Ca} activation does not occur in MSMCs (15). Although a role for this channel in maintaining the membrane potential in MSMCs, and potentially uterine quiescence, throughout pregnancy is well supported (9, 13, 16), BK_{Ca} channel protein

Significance

The large-conductance, voltage-gated, calcium (Ca^{2+})-activated potassium channel (BK_{Ca}) plays an important role in regulating the membrane potential of uterine muscle cells. We demonstrate that BK_{Ca} interacts with the immunomodulator α-2-macroglobulin (α_2M) and its receptor low-density lipoprotein receptor-related protein 1 in human uterine muscle cells isolated from pregnant women. Furthermore, we report that activated α_2M regulates BK_{Ca} activity and that activated α_2M and BK_{Ca} together control Ca^{2+} oscillations in the cells, a process dependent on store-operated Ca^{2+} entry. This study reveals a previously unidentified modulator of the BK_{Ca} channel and may imply a link between inflammatory processes and excitation changes in the uterine muscle during pregnancy.

Author contributions: M.W.-P., R.A.L., X.M., M.E.W., and S.K.E. designed research; M.W.-P., R.A.L., X.M., S.J.S., C.A., and J.J.H. performed research; C.M.K. and K.L.H. contributed new reagents/analytic tools; M.W.-P., R.A.L., X.M., S.J.S., J.J.H., K.L.H., M.E.W., and S.K.E. analyzed data; and M.W.-P., R.A.L., X.M., J.J.H., M.E.W., and S.K.E. wrote the paper.

The authors declare no conflict of interest.

This article is a PNAS Direct Submission.

[1]To whom correspondence should be addressed. Email: englands@wustl.edu.

This article contains supporting information online at www.pnas.org/lookup/suppl/doi:10.1073/pnas.1516863113/-/DCSupplemental.

expression is lower in myometrial biopsies isolated from women at term than in biopsies obtained from nonpregnant women (17). Additionally, laboring MSMCs have constitutively active BK_{Ca} channels in the absence of two key channel activators: high levels of Ca^{2+} and depolarizing stimuli (18). These findings indicate that we do not fully understand how BK_{Ca} is regulated throughout pregnancy. One strong possibility is that BK_{Ca} is regulated by association with other proteins. In fact, BK_{Ca} interacts with various plasma membrane and intracellular proteins and acts as a "coordinator" of cell signaling in other tissues (19–23). Such interactions add functional diversity to BK_{Ca} and may contribute to its cell- and tissue-specific regulation.

To identify proteins that interact with BK_{Ca} in human myometrium during pregnancy and assess their roles in uterine excitability, we affinity-purified BK_{Ca} channels from myometrium isolated from women at term and performed a proteomic analysis of the interacting proteins. We focused on a strong "hit" from this screen, the pan-proteinase inhibitor α-2-macroglobulin (α_2M), for three reasons: (*i*) α_2M plasma levels rise consistently and significantly increase during pregnancy (24); (*ii*) α_2M regulates cytokine production, which has been implicated in preterm and term labor (25); and (*iii*) α_2M is important for other aspects of pregnancy, including embryo implantation, in the mouse (26). However, α_2M's role in human pregnancy and labor is not yet known. In its inactive form, α_2M can bind to certain cytokines or proteases, leading to proteolytic digestion of the "bait" region of α_2M and trapping of the cytokine/proteases. The proteolytic digestion conformationally changes α_2M to its active form (α_2M*), a state in which it can inhibit the bound endoprotease. This change also exposes the receptor recognition site/epitope for high-affinity binding to the α_2M* receptor, low-density lipoprotein receptor-related protein 1 (LRP1) [reviewed in Rehman et al. (27)]. Binding of α_2M* to LRP1 initiates endocytosis of the cytokine/protease–α_2M*–LRP1 complex, mediating the clearance of cytokines/proteases (28, 29), and also leads to an increase in $[Ca^{2+}]_i$ (30). Several cell types secrete α_2M, and, given its regulation by multiple factors, including cytokines and hormones (24), this protein may have cell-specific roles.

Here, we demonstrate that the BK_{Ca} channel associates with α_2M and its receptor LRP1 in hMSMCs. Electrophysiological measurements show that in the presence of OXT, α_2M* induces oscillatory increases in the open-state probability of the BK_{Ca} channel. Ca^{2+} imaging studies show that α_2M* binding to LRP1 induces Ca^{2+} oscillations and Ca^{2+} influx through store-operated Ca^{2+} channels (SOCs) in OXT-primed cells. Furthermore, BK_{Ca} channel activity can regulate the Ca^{2+} oscillations induced by α_2M*. Our findings that α_2M* regulates the BK_{Ca} channel and myometrial $[Ca^{2+}]_i$ dynamics provide evidence that immune-modulating signaling pathways interact with controllers of myometrial excitability.

Materials and Methods

Tissue Samples. Human myometrial tissue samples from the lower uterine segment were obtained from nonlaboring women at term (≥37 wk gestation) during elective Cesarean section under spinal anesthesia. The recruited subjects had a history of repeat Cesarean sections with no spontaneous or induced labor. A total number of 105 myometrial biopsies were used for these studies. All subjects signed written consent forms approved by the Washington University in St. Louis Internal Review Board (approval no. 201108143). Tissues were obtained in 0.9% saline solution and processed within 1 h.

Isolation and Primary Culture of hMSMCs. The hMSMCs were isolated and cultured as previously described (31). Briefly, the tissue was washed twice in cold Dulbecco's PBS containing 50 μg/mL gentamicin and 5 μg/mL Fungizone (both from GIBCO-BRL). The tissue was then cut into 2- to 3-mm pieces, and explants were cultured in DMEM-Ham's F-12 medium supplemented with 5% FBS, 25 μg/mL gentamicin, 2 ng/mL basic FGF, 3 ng/mL EGF (Lonza), 5 μg/mL Fungizone, and 5 μg/mL insulin (Sigma). Once explant colonies formed, they were expanded. For all experiments, hMSMCs were used at passage 1 or 2.

Protein Preparation from Tissues. For total lysate (TL) preparations, human nonlaboring uterine tissue was homogenized in Triton-lysis buffer [1% Triton, 150 mM NaCl, 10 mM Tris (pH 8.0)] plus a complete protease inhibitor tablet (Roche) as previously described (32), and then spun at 800 × *g* for 15 min. The supernatant was cleared by spinning at 14,000 × *g* for 15 min. Isolation of membrane proteins followed the same procedure except that membrane preparation (MP) buffer [250 mM sucrose, 50 mM 3-morpholinopropane-1-sulfonic acid, 2 mM EDTA, 2 mM EGTA (pH 7.4)] was used, and the final supernatant was further centrifuged at 54,000 × *g* for 80 min. The pellet was then resuspended overnight with gentle agitation in 100–200 μL of Triton lysis buffer. All steps were performed at 4 °C.

Cross-Linking Abs to Beads. Abs against BK_{Ca} (rabbit polyclonal; Santa Cruz Biotechnology), LRP1 (mouse monoclonal; Santa Cruz Biotechnology), α_2M (mouse monoclonal, R&D Systems), and rabbit and goat IgG (Sigma) were incubated with protein A/G beads (Santa Cruz Biotechnology) at room temperature for 1 h. The beads were pelleted at 1,000 × *g* for 2 min at 4 °C, washed three times with 0.01 M PBS (pH 7.5), and then incubated in 450 μM disuccinimidyl suberate (DSS; Pierce) in anhydrous dimethyl formamide for 1 h at room temperature. Beads were pelleted, and DSS was quenched by washing the beads in 50 mM Tris·HCl (pH 7.5) for 15 min at room temperature. After washing with 0.01 M PBS, the beads were suspended in 100 μL of 0.01 M PBS containing 0.025% sodium azide.

Affinity Purification and Sample Preparation for MS. Myometrial tissue MP samples (200 μg) were precleared with protein A/G beads for 30 min at room temperature and then incubated with anti-BK_{Ca}– or rabbit IgG-coupled beads overnight at 4 °C in immunoprecipitate (IP) buffer [1% Triton X-100, 150 mM NaCl, 10 mM Tris (pH 7.5)] containing 100 mM PMSF. The lysate–Ab–bead complexes were washed three times with washing buffer [0.5% Triton X-100, 150 mM NaCl, 1 mM EDTA, 50 mM Tris·HCl (pH 7.5)], and the protein–Ab complexes were eluted from the beads with a 1 × 100-μL wash of 100 mM Gly (pH 2.5) and 2 × 100-μL washes of 100 mM Gly and 3 M urea (pH 2.5) at room temperature. Samples were neutralized with 1 M Tris at pH 8.0. The samples were dialyzed against 50 mM Tris and 8 M urea (pH 8.5), and buffer-exchanged two more times with 400 μL of 50 mM Tris at pH 8.0. Proteins were reduced in 10 mM DTT for 1 h at 37 °C, alkylated in 55 mM iodoacetamide (Thermo Scientific) for 1 h at room temperature in the dark, and digested overnight with 1 μg of trypsin gold (Promega) in 1 M urea. Each sample was spiked with a tryptic digest of BSA containing iodoacetic acid alkylated Cys residues (Michrom Bioresources) at a ratio of 1:75. Samples were acidified and desalted on Vydac C18 spin-columns (The Nest Group) and subjected to strong-cation exchange (SCX) fractionation on polysulfoethyl-A packed spin columns (The Nest Group) according to the manufacturer's protocol. Briefly, desalted samples were dissolved into SCX buffer A [5 mM $KHPO_4$, 25% acetonitrile (ACN)] and loaded onto SCX spin-columns, and the tryptic digests were released from the SCX spin-columns by a three-step (20 mM, 40 mM, 60 mM) KCl elution gradient made from a mixture of SCX buffer A and SCX buffer B (5 mM $KHPO_4$, 25% ACN, 350 mM KCl). Salt-bumped eluted fractions were desalted on C18 microspin-columns (The Nest Group), dried down, and dissolved into MS loading buffer (1% acetic acid, 1% ACN).

MS. Samples were subjected to liquid chromatography/tandem MS (LC-MS/MS) on an Agilent 6520 Accurate-Mass Quadropole Time-of-Flight mass spectrometer (Agilent Technologies) interfaced with an HPLC Chip Cube. The samples were loaded onto the large-capacity C18 Chip II (160-nL enrichment column, 9-mm analytical column) and subjected to LC-MS/MS analysis using a 60-min gradient from 1.5% to 35% buffer B (100% ACN, 0.8% acetic acid). The data-dependent settings (MS/MS) included a maximum of 10 ions per cycle at medium isolation width [~4 atomic mass units (AMU)], and precursor masses were dynamically excluded for 30 s after five MS/MS in a 30-s time window. MS capillary voltage and temperature settings were set to 1,800 V and 330 °C, respectively.

Data Analysis-Spectrum Mill Analysis. The raw.d files were searched against the UniProt human database using Spectrum Mill software, version B.04.00.127 (Agilent Technologies) with the following settings: precursor mass tolerance of 50 ppm, product mass tolerance of 300 ppm, and a maximum of two trypsin miscleavages. The search modifications included a static carbamidomethylation on Cys residues (C = 57.02146 AMU) and the following posttranslational modifications: oxidized methionine (M = 15.9949 AMU), phosphorylated Ser, Thr, and Tyr (STY = 79.9663 AMU), and ubiquitinated Lys (K = 114.0429 AMU).

Coimmunoprecipitation for Western Blotting. MP and TL protein samples (200 μg) in 200 μL of IP buffer [10 mM Tris, 150 mM NaCl, 1% Triton X-100,

1 mM PMSF (pH 7.5)] were preadsorbed to 40 μL of Protein A/G beads for 30 min at 4 °C. The preadsorbed samples were then incubated with 60 μL of Ab cross-linked beads overnight at 4 °C with gentle agitation. The beads were pelleted at 1,200 × *g* for 2 min at 4 °C, washed for 3 × 5 min with Wash Buffer-A [0.5% Triton X-100,150 mM NaCl, 50 mM Tris·HCl, 1 mM EDTA (pH 7.5)], and eluted with 80 μL of 2× SDS buffer (for BK_{Ca} and α_2M Abs) or 100 mM Gly at pH 2.5 (for LRP1 Ab). Samples were resolved on 4–15% gradient gels and transferred to nitrocellulose membranes. Blots were blocked in 5% (wt/vol) nonfat dry milk in TBS-Tween 20 and probed with Abs against LRP1 (1:400) or α_2M (1:1,500) in blocking buffer overnight at 4 °C. Blots were washed in TBS-Tween at room temperature, probed with secondary anti-mouse or anti-goat Abs (1:10,000; Jackson Immunoresearch) for 1 h at room temperature, and developed with enhanced chemiluminescence (Denville Scientific Inc.).

In Situ Proximity Ligation Assay. The hMSMCs were cultured in chambered slides (eight-well; LabTek), serum-deprived in 0.5% FBS for 24 h, washed with ice-cold PBS, and then fixed in 4% (wt/vol) paraformaldehyde (PFA) in PBS for 30 min at room temperature with gentle rocking. After 3 × 5-min washes in 0.01 M PBS, cells were permeabilized with 0.1% Triton X-100 for 15 min at room temperature, washed twice with PBS, and washed once in PBS containing 100 mM Gly to quench residual PFA. The slides were rinsed in milliQ water to remove residual salts, and in situ proximity ligation assay (PLA; Duolink PLA; Olink Biosciences) labeling was performed with Abs against the following proteins: BK_{Ca}, β1 (rabbit polyclonal; Abcam), α_2M, LRP1, and the small-conductance Ca^{2+}-activated K^+ channel (SK3, rabbit monoclonal; Alomone Labs) (all diluted 1:100 except for LRP1, which was diluted 1:250). The manufacturer's protocol was followed exactly except that the cells were stained with nuclear dye TOPRO 3-iodide (1:1,000; Invitrogen) for 5 min at room temperature before the final wash in wash buffer B. Slides were dried at room temperature in the dark, mounted in Vectashield (Vector Laboratories), and stored in the dark at −20 °C until they were analyzed by confocal microscopy (FV500; Olympus). PLA signals were detected at 563 nm, and TOPRO 3-iodide was detected at 633 nm. Duolink ImageTool software (Olink Biosciences) was used for analysis. For accuracy of the quantitation, in certain images, clustered nuclei or nonspecific pixels outside the cells' boundary were digitally removed before analysis. All data are presented as mean ± SEM.

Activation of α_2M. For some experiments, α_2M (Sigma) was activated by incubation in 100 mM methylamine (Sigma) in 0.01 M PBS (pH 7.5) for 1 h at room temperature. Activated α_2M (α_2M*) was then dialyzed in at least three changes of PBS over 24 h at 4 °C as described previously (30). Inactive α_2M was processed identically except that methylamine was excluded. For other experiments, α_2M* was purchased from BioMac (no. 05-04). No differences in Ca^{2+} imaging data or patch-clamp recordings were observed between these two sources of α_2M*.

Electrophysiology. Whole-cell patch-clamp recordings were performed on hMSMCs at room temperature in a bath solution containing 135 mM NaCl, 4.7 mM KCl, 5 mM Hepes, 10 mM glucose, 1 mM $MgCl_2$, and 2 mM Ca^{2+} (pH 7.4); the pipette solution contained 140 mM KCl, 0.5 mM $MgCl_2$, 10 mM Hepes, 1 mM EGTA, and 5 mM Mg-ATP (pH 7.2). Currents were elicited with 20-mV steps (100 ms) from −100 mV to +100 mV, from a holding potential of −80 mV, and were acquired at a sampling rate of 1 kHz using an Axopatch 200B amplifier and pCLAMP software (Molecular Devices). Currents were recorded, in the same cell, in the presence of 350 nM α_2M and after superfusion with 350 nM α_2M* for 3 min. Current densities (picoamperes/picofarads) were plotted as a function of membrane potential.

Single-channel recordings in the cell-attached configuration were performed at room temperature on hMSMCs in a bath solution containing 135 mM NaCl, 4.7 mM KCl, 5 mM Hepes, 10 mM glucose, 1 mM $MgCl_2$, and 2 mM Ca^{2+} (pH 7.4). Pipette solution contained 140 mM KCl, 20 mM KOH, 2 mM $MgCl_2$, and 10 mM Hepes (pH 7.2). Single-channel currents were recorded for 20 min before adding 100 nM OXT; then, after 10 min, either 350 nM α_2M or α_2M* was added to the recording chamber, and currents were acquired for at least another 30 min. A holding potential of +100 mV was maintained during the whole experiment. Recordings were acquired at 100 kHz and filtered at 5 kHz. Open probability (P_o), open dwell-time, and single-channel conductance were calculated for each condition using pCLAMP software (Molecular Devices).

Ca^{2+} Imaging. The hMSMCs were loaded with 4 μM Fura-2-AM (Teflabs) and 0.1% Pluronic F-127 (Invitrogen) for 30 min at room temperature in the dark in the following buffer: 140 mM NaCl, 5.4 mM KCl, 0.8 mM $MgCl_2$, 1.8 mM $CaCl_2$, 10 mM NaOH, 10 mM Gly, 10 mM Hepes, 5.5 mM glucose, and 1.1 mM Na_2HPO_4 (pH 7.4). Cells were then washed with buffer devoid of fluorophore and incubated for an additional 40 min at room temperature to allow de-esterification of Fura-2-AM. The cells were then imaged on an inverted iMIC digital microscope (Till Photonics) using a 20×/0.75 objective (Olympus). The fluorescence excitation was provided by a Polychrome V monochromator (Till Photonics). A CCD camera (Cooke) was used to collect paired images at alternating excitation wavelengths (340/380 nm) through a 510-nm emission filter at 2.608-s intervals. After subtracting the matching background, the image intensities were divided by one another to yield ratio values for individual cells. Free cytosolic calcium concentration, $[Ca^{2+}]_i$, was estimated in individual cells according to the formula

$$[Ca^{2+}]_i = K_d * B * (R - R_{min})/(R_{max} - R),$$

where K_d is the indicator's dissociation constant for Ca^{2+} (0.22 μM), R is ratio of fluorescence intensity at two different wavelengths (340/380 nm), R_{max} and R_{min} are the ratios of Ca^{2+}-free and Ca^{2+}-bound fura-2, respectively, and B is the ratio of the fluorescence intensity of the second excitation wavelength at zero and saturating Ca^{2+} concentrations (33). The calibration constants (R_{min}, R_{max}, and B) were determined on the same setup in calibration buffers (Invitrogen) containing Fura-2/K^+ and either 10 mM EGTA or 39.6 μM free Ca^{2+}.

For Ca^{2+} imaging studies, 100 nM OXT and 350 nM α_2M or α_2M* were added to the hMSMCs, and $[Ca^{2+}]_i$ was measured for at least 45 min. To test desensitization of the OXT receptor, 100 nM OXT was added a second time. Some measurements were taken in the presence of (*i*) nominal Ca^{2+} buffer (Ca^{2+}-free), (*ii*) the L-type Ca^{2+} channel blocker nifedipine (20 μM; Sigma), or (*iii*) the broadly acting SOC blocker 2-aminoethoxydiphenylborane (2-APB, 40 μM) or *N*-[4-[3,5-*Bis*(trifluoromethyl)-1*H*-pyrazol-1-yl]phenyl]-4-methyl-1,2,3-thiadiazole-5-carboxamide (BTP2, 1 μM) (Tocris Biosciences). In some experiments, MSMCs were pretreated for 1 h with 40 μM 2-APB, 1 μM BTP2, or the inositol 1,4,5-triphosphate (IP_3) receptor inhibitor xestospongin C (10 μM; Tocris Biosciences). In another set of experiments, cells were pretreated with 500 nM of the LRP1 antagonist receptor-associated protein (RAP; Millipore) for 1 h before stimulation with OXT and α_2M*. Some of the Ca^{2+} recordings were performed in the presence of the BK_{Ca} selective blocker paxilline (500 nM; Tocris Biosciences) or opener NS11021 (500 nM; Glixx Laboratories), which were added to the cells after the oscillations were observed. The cells that did not respond to OXT and failed to produce rhythmic Ca^{2+} spikes after α_2M* stimulation were excluded from the data analysis in each experimental condition. All of the drugs tested were added to the media and remained in the recording chamber until the end of the experiments, with the exception of paxilline reversibility experiments, where the media in the chamber were replaced. The frequency of Ca^{2+} oscillations was measured as the time between consecutive peaks and was represented as the number of oscillations per hour. GraphPad Prism 6 software was used for data analysis. Replicates are expressed as number of cells and number of tissue samples.

Results

α_2M Is Expressed in Human Myometrium and Interacts with BK_{Ca}. To identify proteins that interact with BK_{Ca} in myometrium from pregnant women, we generated TLs and MPs from term nonlabor human myometrial tissues and used a BK_{Ca}-specific Ab to affinity purify the BK_{Ca} channel and any interacting proteins. LC-MS/MS analysis of purified samples revealed several proteins known to interact with the BK_{Ca} channel, including the auxiliary β1 subunit, filamin-A, and caveolin-1 (18, 32, 34, 35). In addition, we identified human α_2M (UniProt ID no. P01023) as one of the top five multipeptide hits in the screen. Importantly, α_2M was not detected in negative control samples (tissue purified with IgG). Spectrum Mill software identified eight distinct peptides that covered 5.6% of the α_2M protein (84 of 1,474 amino acids) and 10 peptides that covered 8.4% of the BK_{Ca} protein (Table 1). The spectrum of the highest intensity α_2M peptide (MVSGFIPLKPTVK) is shown in Fig. S1.

To confirm the interaction between BK_{Ca} and α_2M, we first verified that α_2M is expressed in human myometrial tissues. Reverse transcriptase quantitative PCR analysis revealed that α_2M, LRP1, and BK_{Ca} mRNAs were all expressed in myometrium samples isolated from term nonlabor and term laboring women. We observed no differences in expression between nonlabor and laboring states (Fig. S2*A*, list of primers used in Table S1). Additionally, immunoblot analysis revealed that α_2M, but not α_2M*, protein was present in nonlabor and laboring

Table 1. BK_{Ca} channel and α_2M peptides identified by affinity purification and LC-MS/MS

Protein	Peptide	MS/MS score	Measured *m/z*	Expected *m/z*
BK_{Ca}	(R)AFFYCK(A)	14.07	418.1946	418.1952
	(K)AHLLNIPSWNWK(E)	12.61	493.6009	493.6002
	(K)EGDDAICLAELK(L)	4.28	667.3141	667.3093
	(R)EWETLHNFPK(V)	9.58	434.2136	434.2116
	(R)GGYSTPQTLANR(D)	5.12	632.8139	632.8101
	(R)IITQMLQYHNK(A)	14.91	463.5819	463.5804
	(R)NLVMPLR(A)	9.96	421.7473	421.7451
	(K)SSSVHSIPSTANR(Q)	7.60	448.2263	448.2241
	(K)VSILPGTPLSR(A)	16.74	570.3386	570.3344
	(K)YGGSYSAVSGR(K)	5.66	552.2580	552.2565
α_2M	(K)AIGYLNTGYQR(Q)	7.84	628.3215	628.3179
	(K)ATVLNYLPK(C)	8.11	509.7963	509.7924
	(K)LPPNVVEESAR(A)	4.60	605.8199	605.8148
	(K)MVSGFIPLKPTVK(M)	12.20	472.9427	472.9377
	(R)QGIPFFGQVR(L)	10.45	574.8145	574.8148
	(R)SSGSLLNNAIK(G)	8.93	552.2998	552.2932
	(R)VGFYESDVMGR(G)	4.61	630.2902	630.2905
	(K)YGAATFTR(T)	9.36	443.7226	443.7207

myometrium (Fig. S2*B*). We next examined the TL and MP samples by immunoblot and found that α_2M was present in both (Fig. 1*A*, input lanes). We then immunoprecipitated BK_{Ca} and confirmed by immunoblot that α_2M coimmunoprecipitated with the BK_{Ca} channel in the MP samples (Fig. 1*A*, BK_{Ca} lanes). However, very little α_2M coprecipitated with BK_{Ca} in the TL samples. Finally, we examined LRP1, the receptor through which α_2M^* acts, and found that it was expressed in human myometrium (Fig. 1*B*, input lanes) and coimmunoprecipitated with the BK_{Ca} channel in both TL and MP samples (Fig. 1*B*, BK_{Ca} lanes). As expected, immunoprecipitations with anti-α_2M Ab (Fig. 1*A*, α_2M lanes) and anti-LRP1 Abs (Fig. 1*B*, LRP1 lanes) pulled down their respective targets in both TL and MP samples, whereas immunoprecipitations with IgG did not pull down either protein (Fig. 1 *A* and *B*, IgG lanes).

We further validated these molecular interactions by performing in situ PLAs (36) on hMSMCs. Punctate red fluorescent signals were detected when cells were exposed to Abs specific to BK_{Ca} plus α_2M or BK_{Ca} plus LRP1 (Fig. 1*C*), indicating that these pairs of proteins were located within 40 nM of each other. Signals were not detected in control experiments in which a single Ab was used. As expected, the Ab combinations of BK_{Ca} plus its auxiliary β1 subunit and α_2M plus LRP1 produced signals (Fig. 1*C*). Consistent with the idea that the interaction with LRP1 was specific for the BK_{Ca} channel, PLA using the Ab combination of SK3 channel (another prevalent potassium channel in hMSMCs) and LRP1 produced very few punctae (Fig. 1 *C* and *D*). Together, these data confirm that α_2M and LRP1 are expressed in hMSMCs and interact with the BK_{Ca} channel.

α_2M^* Increases the P_o of BK_{Ca} in hMSMCs. We next evaluated the functional significance of the interaction between BK_{Ca} and α_2M by performing whole-cell patch-clamp recordings in the presence of inactive or activated α_2M (α_2M or α_2M^*, respectively). In this recording configuration, neither α_2M^* nor α_2M significantly affected the BK_{Ca} current over a voltage range from −100 to +100 mV (Fig. 2*A*). Previous studies have shown that α_2M^* increases $[Ca^{2+}]_i$ (30, 37, 38), a key regulator of the BK_{Ca} channel. Thus, we used the single-channel, cell-attached, patch-clamp configuration, in which cell constituents and signaling pathways are intact, to investigate whether α_2M^* regulates BK_{Ca} activity. Under control conditions, hMSMCs showed low levels of BK_{Ca} channel activity (Fig. 2 *B* and *C*). To ensure that cells were able to release $[Ca^{2+}]_i$, and thereby promote BK_{Ca} channel activation, cells were superfused with a high dose (100 nM) of the uterotonin OXT. At this dose, OXT increases $[Ca^{2+}]_i$ via G protein-coupled receptor activation and release of diacylglycerol and IP_3, and rapidly desensitizes the OXT receptors (39). Of the cells tested, 49% (36 of 74 cells from 16 myometrial samples) were sensitive to OXT. In these cells, OXT

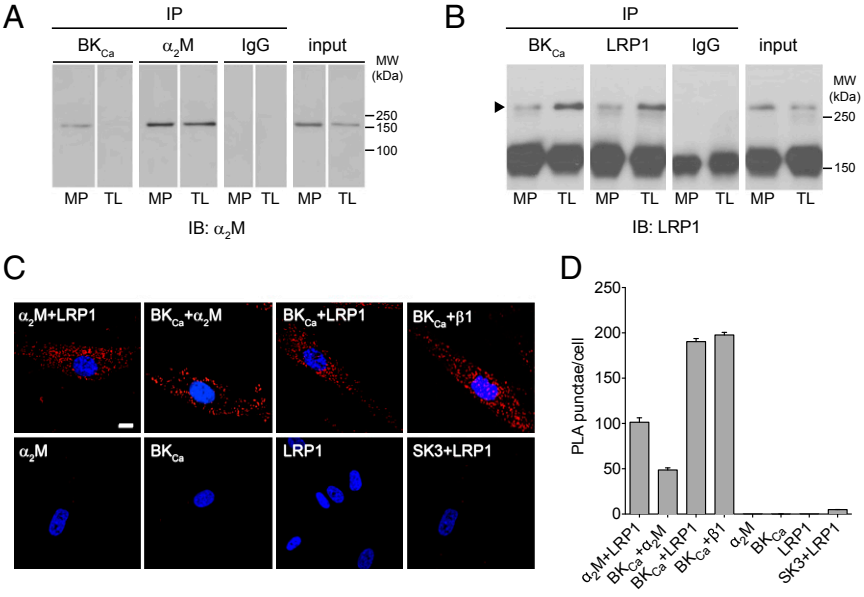

Fig. 1. BK_{Ca} channel associates with α_2M and LRP1 in human myometrium and hMSMCs. (*A* and *B*) Representative immunoblots (IBs) of immunoprecipitates (IPs) of MPs and TLs from myometrial tissue from pregnant women. Immunoprecipitation was performed with Abs against the indicated proteins, and blots were probed with Abs specific to α_2M (*A*) and LRP1 (*B*). α_2M was detected at ∼180 kDa (*A*, SDS/PAGE), and LRP1 was detected at ∼500 kDa (arrow in *B*, native PAGE). The ∼150-kDa band in *B* is IgG. MW, molecular weight. (*C*) Representative PLA labeling of hMSMCs with the indicated single Abs and Ab combinations. (Scale bar, 10 μm.) (*D*) Average number of PLA signals in cells is as in *C*. Error bars indicate SEM (n = 200 each).

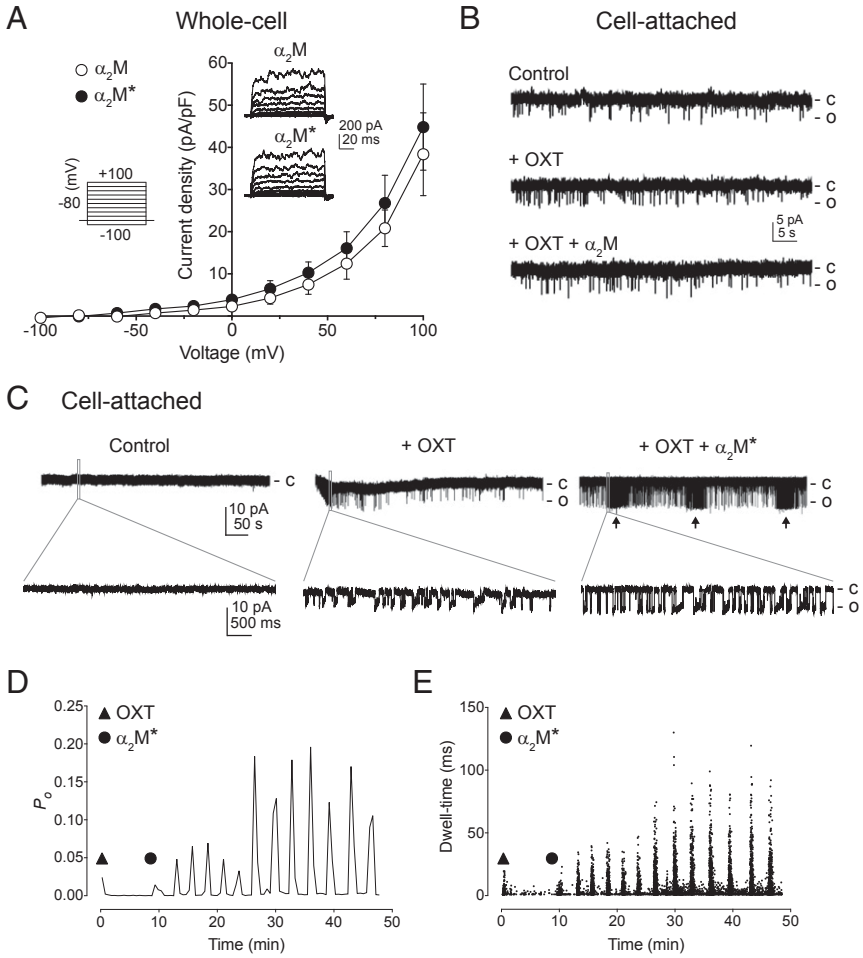

Fig. 2. α_2M* causes oscillatory increases in BK_{Ca} channel activity in hMSMCs. (*A*) Plots of whole-cell current densities in hMSMCS evoked from −100 mV to +100 mV in 20-mV steps from a holding potential of −80 mV in the presence of 350 nM α_2M* (●) or α_2M (○) ($n = 6$). (*Insets*) Voltage-step protocol and representative recordings. (*B–E*) Representative cell-attached BK_{Ca} single-channel currents evoked by +100 mV, with 160 mM K^+ in the pipette, in hMSMCs before and after addition of 100 nM OXT and 350 nM α_2M (*B*) or 100 nM OXT and 350 nM α_2M* (*C*). Arrows indicate phasic increases in BK_{Ca} currents. c, closed state of channels; o, open state of channels. (*D* and *E*) Single-channel analysis of P_o (*D*) and open dwell-time (*E*) of the BK_{Ca} channel in the presence of OXT and α_2M* ($n = 10$).

induced an increase in the P_o and dwell-time (from 1.29 to 4.47 ms) of the BK_{Ca} single-channel currents (Fig. 2 *B* and *C*). Treatment of hMSMCs with inactive α_2M did not alter P_o or dwell-time (Fig. 2*B*; 0 of 12 cells from six myometrial samples responded to α_2M). In contrast, 28% (10 of 36 cells from 16 myometrial samples) of cells responded to application of α_2M* by increasing both P_o and dwell-time of the BK_{Ca} channel openings. However, these increases were oscillatory (19.12 ± 4.85 oscillations per hour; Fig. 2 *C–E*). These results indicate that α_2M* activates BK_{Ca} channels, likely through intracellular pathways.

The Interaction of α_2M* with LRP1 Leads to Ca^{2+} Oscillations in hMSMCs. Given the observations that α_2M* can cause an increase in $[Ca^{2+}]_i$ in osteoblasts (37), macrophages (38), and mouse cortical neurons (30), and the fact that $[Ca^{2+}]_i$ regulates BK_{Ca} activity, we wondered whether α_2M* causes an increase in $[Ca^{2+}]_i$ in hMSMCs. To examine this possibility, we used the Ca^{2+}-sensitive dye Fura-2-AM to measure $[Ca^{2+}]_i$ in hMSMCs (Fig. S3 and Table S2). We first confirmed that the cells were able to respond to OXT, which is known to increase $[Ca^{2+}]_i$. Addition of 100 nM OXT induced a short-duration (Fig. 3*A*; 4 ± 1.5 min) single-spike increase in $[Ca^{2+}]_i$ in ∼80% (901 of 1,127) of the cells analyzed. Although OXT was present throughout the entire experiment, it did not evoke any further response for up to 100 min. This was likely due to desensitization of the OXT receptor, because a second application of 100 nM OXT failed to produce any increase in $[Ca^{2+}]_i$ (Fig. 3*A*). When 350 nM α_2M* was applied after OXT, we observed Ca^{2+} oscillations at regular time intervals (Fig. 3*B* and Table 2). Whereas the baseline free $[Ca^{2+}]_i$ of the hMSMCs was 20.9 ± 13 nM, the α_2M*-induced $[Ca^{2+}]_i$ peaks were 298 ± 0.08 nM (Table 2). We did not observe α_2M*-induced Ca^{2+} oscillations in cells treated with α_2M* in the absence of OXT (Fig. 3*C*).

To determine whether α_2M* acted through its receptor, LRP1, we pretreated hMSMCs with 500 nM RAP, a competitive antagonist of LRP1. In this case, the amplitude of the initial OXT-induced short-duration increase in $[Ca^{2+}]_i$ was reduced and the α_2M*-induced Ca^{2+} oscillations did not occur (Fig. 3*D*). Furthermore, inactive α_2M, which is unable to bind to LRP1, did not induce any change in $[Ca^{2+}]_i$ (Fig. 3*E*).

To identify the source of Ca^{2+}, we measured $[Ca^{2+}]_i$ in the absence of extracellular Ca^{2+} (Ca^{2+}-free buffer). Under these conditions, α_2M* was unable to produce oscillations, although the OXT-elicited peak of $[Ca^{2+}]_i$ still occurred (Fig. 4*A*). Next, we assessed whether the Ca^{2+} entered the cytoplasm through L-type Ca^{2+} channels, a major source of Ca^{2+} entry in MSMCs; through the sarcoplasmic reticulum; or by SOCE. Treating the cells with the L-type Ca^{2+} channel blocker nifedipine did not affect the oscillations (Fig. 4*B*). However, α_2M* was not able to elicit Ca^{2+} oscillations when hMSMCs were pretreated with either of two SOCE

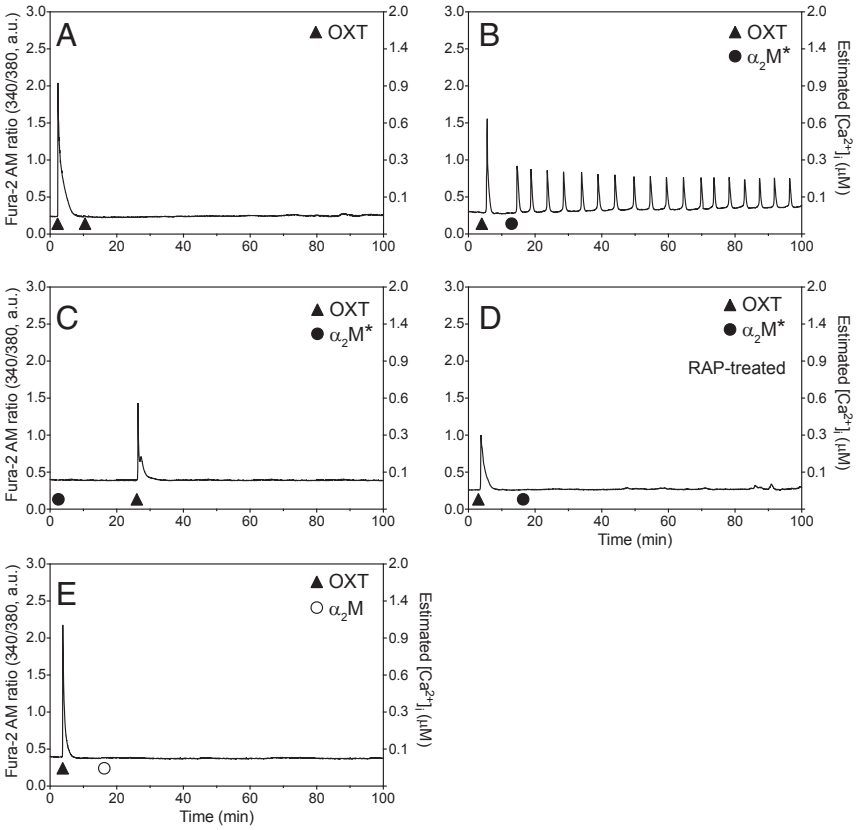

Fig. 3. α_2M* induces $[Ca^{2+}]_i$ oscillations in OXT-primed hMSMCs by binding LRP1. Representative live-cell Ca^{2+} imaging recordings of Fura-2-AM–loaded hMSMCs are shown. An increase in $[Ca^{2+}]_i$ is reported as a ratiometric measure of Fura-2-AM fluorescence at 340/380 nm [in arbitrary units (a.u.)], with background subtraction (*Left*, *y* axis) and estimated $[Ca^{2+}]_i$ concentration (*Right*, *y* axis) (details are provided in *Materials and Methods*). In all experiments, 100 nM OXT (▲) was added at the indicated times. (*A*) Only OXT was added. (*B*) α_2M* (●; 350 nM) was added after OXT. (*C*) α_2M* (350 nM) was applied before 100 nM OXT. (*D*) Cells were incubated with 500 nM RAP, a selective antagonist of LRP1, before OXT, and α_2M* was then added. (*E*) Inactive α_2M (○) was added after OXT.

inhibitors, 40 μM 2-APB or 1 μM BTP2, although the OXT response still occurred (Fig. 4 *C* and *E*). Moreover, adding either 40 μM 2-APB or 1 μM BTP2 after α_2M*-induced Ca^{2+} oscillations were established abolished these oscillations, although the effect of BTP2 was slower than the effect of 2-APB (Fig. 4 *D* and *F*). Finally, blocking IP_3 receptors on the sarcoplasmic reticulum with xestospongin C inhibited both the OXT response and the Ca^{2+} oscillations (Fig. 4*G*). Together, our data indicate that in hMSMCs primed with OXT, α_2M*-induced Ca^{2+} oscillations require α_2M* binding to its receptor and influx of extracellular Ca^{2+} through SOCs.

BK_{Ca} Activity Modulates the α_2M*-Induced Ca^{2+} Oscillations. In hMSMCs, Ca^{2+} influx depolarizes the plasma membrane and activates BK_{Ca} channels to restore the membrane potential. To determine whether BK_{Ca} activity affected the Ca^{2+} oscillations, we examined the effect of treating the cells with paxilline, a specific BK_{Ca} channel blocker, or NS11021, a specific BK_{Ca} channel opener. When 500 nM paxilline was added to the cells after establishment of α_2M*-induced Ca^{2+} oscillations, the oscillations were completely abolished (Fig. 5*A* and Table 2). This result was surprising because we assumed that paxilline would induce depolarization and increase the frequency of the Ca^{2+} oscillations. In fact, we observed no change in $[Ca^{2+}]_i$ after paxilline was added in the absence of α_2M* (Fig. 5*C*) or in the presence of inactive α_2M (Fig. S4*A*). In contrast, addition of 500 nM NS11021 increased the frequency of the oscillations by twofold (Fig. 5*B* and Table 2). NS11021 did not affect $[Ca^{2+}]_i$ in the absence of α_2M* (Fig. 5*D*) or in the presence of inactive α_2M (Fig. S4*B*). To determine whether the Ca^{2+} oscillations could be recovered, paxilline was washed out and replaced with buffer

Table 2. Effect of BK_{Ca} modulators on α_2M*-induced Ca^{2+} oscillations

Agents added after OXT†	Percentage of α_2M*-responsive cells‡	Fura-2 ratio (340 of 380)§	Estimated peak $[Ca^{2+}]_i$, nM§	Frequency, oscillations per hour§
α_2M*	62.25 (127/204)	0.98 ± 0.07	298 ± 0.08	11 ± 0.78
α_2M*; paxilline	60.38 (32/53)	0	0	0
α_2M*; NS11021	62.5 (35/56)	0.93 ± 0.72	281 ± 0.09	20 ± 0.81¶

†Agents are listed in order added and separated by semicolons.
‡n = 43 patients.
§Mean ± SEM.
¶$P < 0.05$ compared with α_2M*.

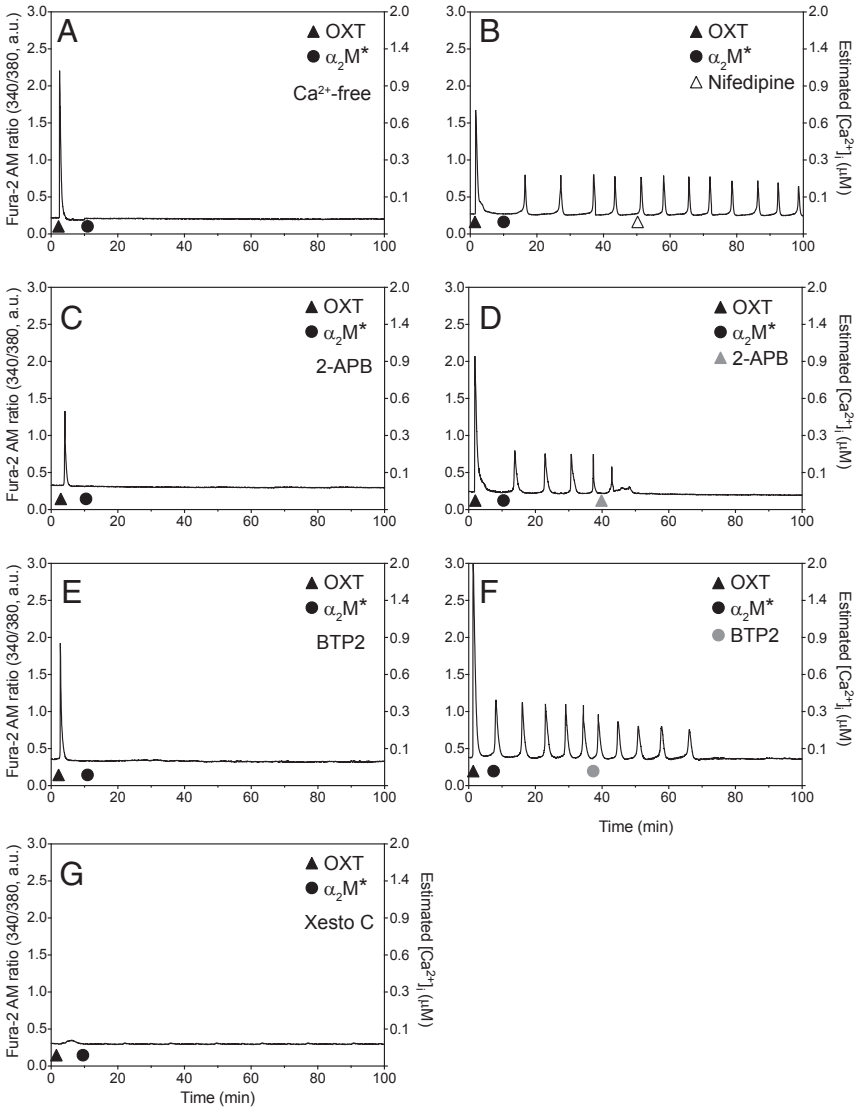

Fig. 4. Ca^{2+} oscillations evoked by α_2M^* in hMSMCs require extracellular Ca^{2+} entry through SOCs. (*A*–*G*) Representative live-cell Ca^{2+} imaging recordings of Fura-2-AM–loaded hMSMCs. (*A*) Cells were preincubated in Ca^{2+}-free extracellular medium before addition of OXT (▲) and α_2M^* (●). (*B*) L-type Ca^{2+} channel blocker nifedipine (△) was added after OXT and α_2M^*. Cells were preincubated with the SOC inhibitor 2-APB (*C*) or BTP2 (*E*) before addition of OXT and α_2M^*. The 2-APB (*D*, gray triangle) or BTP2 (*F*, gray circle) was added after OXT and α_2M^*. (*G*) Cells were pretreated with the IP_3 receptor antagonist xestospongin C (Xesto C) before addition of OXT and α_2M^*.

containing OXT and α_2M^*. In ∼30% of cells, the Ca^{2+} oscillations returned, although they showed reduced amplitude (Fig. S5 and Table S3). Reapplication of OXT plus α_2M^* (in the absence of paxilline) did not affect the already initiated α_2M^*-induced Ca^{2+} oscillations (Fig. S5*A*).

Discussion

BK_{Ca} is the predominant K^+ channel transcript in human myometrium (10), but its role in regulating uterine contraction is not well understood. In this study, we used an unbiased affinity purification and LC-MS/MS approach to identify proteins that interact with the BK_{Ca} channel in the human myometrium during pregnancy. This approach revealed an interaction between the BK_{Ca} channel and α_2M. Furthermore, we showed that the BK_{Ca} channel associates with the α_2M receptor, LRP1, in MSMCs from term pregnant women. Thus, we have identified a previously unknown BK_{Ca} channel complex in hMSMCs that may contribute to regulation of myometrial excitation.

Our observations comparing the effects of α_2M and α_2M^* lead us to speculate that the BK_{Ca} channel regulates Ca^{2+} dynamics only in cells in an inflammatory state. For example, we found that pharmacological inhibition or activation of BK_{Ca} did not affect Ca^{2+} dynamics in cells treated with α_2M but abolished or increased, respectively, the frequency of Ca^{2+} oscillations in cells treated with α_2M^*. Furthermore, other studies have shown that paxilline does not affect spontaneous contractions of the uterus (5, 6). On the basis of our data, we formulated the model illustrated in Fig. 6. First, OXT, a key uterotonin released in labor and used clinically for labor induction and augmentation (40), induces an initial rise of $[Ca^{2+}]_i$ through activation of IP_3 receptors (Fig. 6*A*). Second, LRP1 activation by α_2M^* promotes extracellular Ca^{2+} entry via SOCE in conjunction with sarcoplasmic Ca^{2+} release and transient activation of BK_{Ca} channels (Fig. 6*B*). When BK_{Ca} channels are blocked, K^+ efflux is prevented, thus lowering the driving force for Ca^{2+} influx into the cell (Fig. 6*C*). Conversely, pharmacological activation of BK_{Ca} channels facilitates Ca^{2+} influx, thereby increasing the frequency

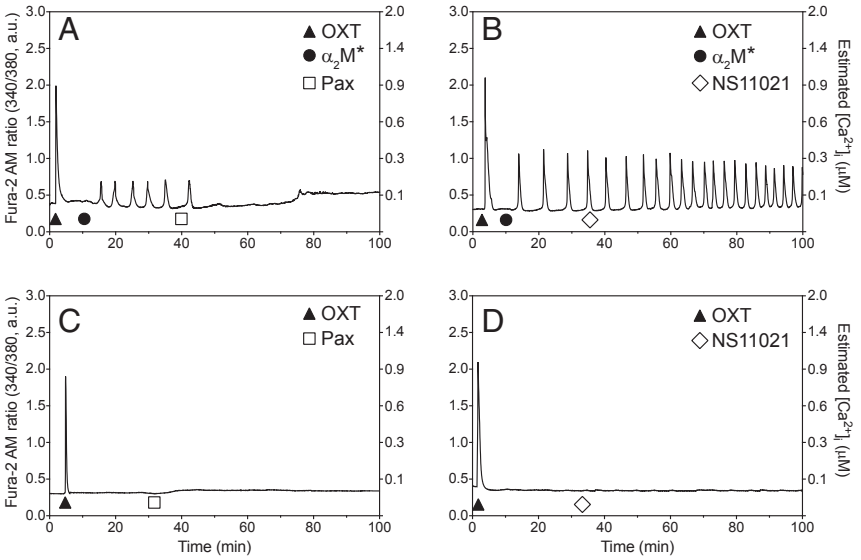

Fig. 5. BK_{Ca} channel modulates α_2M*-induced Ca^{2+} oscillations. Representative live-cell Ca^{2+} imaging recordings of Fura-2-AM–loaded hMSMCs are shown. The specific BK_{Ca} blocker paxilline (Pax) (*A* and *C*, □) or opener NS11021 (*B* and *D*, ◇) was added after OXT (▲) and α_2M* (●). (*C* and *D*) No α_2M* was added.

of α_2M*-elicited Ca^{2+} oscillations (Fig. 6*D*). Our observation that nifedipine did not abolish the α_2M*-induced Ca^{2+} oscillations leads us to speculate that BK_{Ca} activity-induced Ca^{2+} influx is due to SOCE rather than influx of Ca^{2+} through L-type Ca^{2+} channels.

Our findings run somewhat counter to traditional concepts about activity of the BK_{Ca} channel. Opening of the BK_{Ca} channel provides a strong repolarizing current to maintain MSMCs at a polarized membrane potential, thus preventing voltage-gated Ca^{2+} influx and contraction. Conversely, pharmacological block of BK_{Ca} channels depolarizes immortalized myometrial cells, causing activation of voltage-sensitive L-type Ca^{2+} channels and increased $[Ca^{2+}]_i$ (13). However, we found the opposite: In the presence of α_2M*, the channel opener NS11021 stimulated Ca^{2+} oscillations, creating a potentially procontractile state. At resting potential, BK_{Ca} displays a low open-state probability (32), and pharmacological block does not alter uterine activity (6). In light of our findings, we speculate that, depending on the inflammatory state, the BK_{Ca} channel can play two roles in the MSMCs. In a noninflammatory state, BK_{Ca} behaves in a fashion typically noted in excitable cells: The channel is activated at high depolarizing voltages, leading to K^+ efflux, repolarization of the MSMC membrane, and deactivation of voltage-gated Ca^{2+} channels. Conversely, in an inflammatory state, such as we have mimicked with α_2M*, BK_{Ca} activity can regulate Ca^{2+} influx through SOCE to modulate phasic Ca^{2+} oscillations. Inhibition of BK_{Ca} inhibits SOCE, and, conversely, BK_{Ca} activation enhances SOCE. These effects appear to be voltage-independent (given the lack of effect of nifedipine) and are more typical of nonexcitable cells than of excitable cells. In the presence of α_2M*, the effects of paxilline on Ca^{2+} oscillations were immediate, suggesting involvement of plasma membrane BK_{Ca} channels. However, our data do not exclude the possibility that

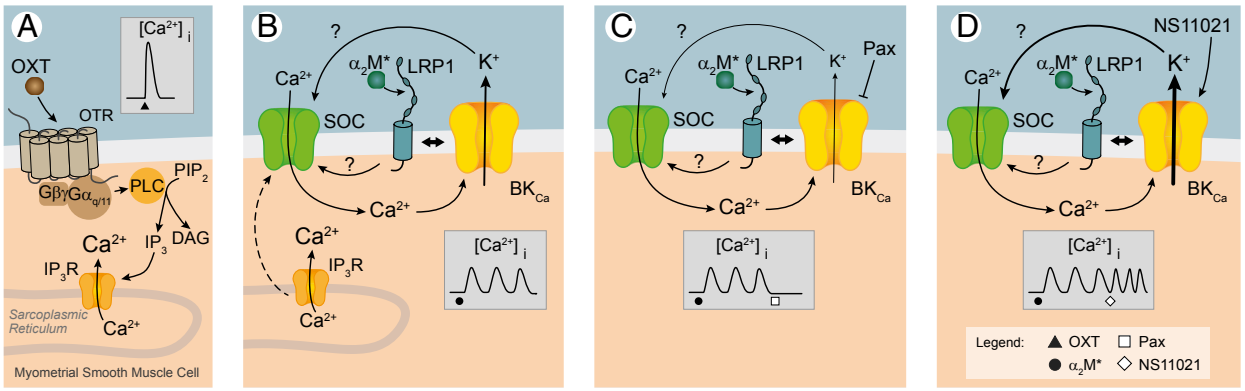

Fig. 6. Working model of Ca^{2+} dynamics regulation by the functional interaction between BK_{Ca} and α_2M*-LRP1 in hMSMCs. (*A*) OXT bound to its receptor induces production of IP_3, which binds its receptor and leads to release of Ca^{2+} from the sarcoplasmic reticulum. (*Insets*) Release is observed as a peak in $[Ca^{2+}]_i$. (*B*) Release of Ca^{2+} from the sarcoplasmic reticulum activates SOCs. In the presence of α_2M* bound to LRP1, SOC activation induces a moderate transient Ca^{2+} influx and activation of BK_{Ca} channels. BK_{Ca} channel activation leads to K^+ efflux, which facilitates further influx of Ca^{2+} through SOCs. This hyperpolarizes the membrane, increasing the driving force for Ca^{2+} entry and inducing the oscillatory rise in $[Ca^{2+}]_i$, as shown in the *Inset*. (*C*) Blocking BK_{Ca} with paxilline prevents K^+ efflux, so $[Ca^{2+}]_i$ is maintained at low levels. (*D*) In the presence of the BK_{Ca} opener NS11021, K^+ efflux is increased, thereby increasing the Ca^{2+} influx rate to maintain the electrochemical gradient. DAG, diacylglycerol; $G\alpha_{q/11}$, α subunit of protein $G_{q/11}$; Gβγ, β and γ subunits of protein G; IP_3R, IP_3 receptor; OTR, OXT receptor; PIP_2, phosphatidylinositol biphosphate; PLC, phospholipase C.

BK_{Ca} channels localized to other intracellular organelles contribute to Ca^{2+} dynamics in MSMCs (41, 42). In light of our findings, the role of the BK_{Ca} channel in Ca^{2+} signaling in hMSMCs should be revisited and considered in the context of other myometrial signaling events.

Regulation of the BK_{Ca} channel by α_2M^* has been implied, but not directly shown, in other studies. For example, serum α_2M induced transient, discrete, hyperpolarizing spikes in isolated cells of a rat osteosarcoma cell line; these spikes were hypothesized to be due to opening of Ca^{2+}-dependent K^+ channels by $[Ca^{2+}]_i$ (37). Our data showing that α_2M^* activates the BK_{Ca} channel likely through increases in $[Ca^{2+}]_i$ rather than by direct activation of the channel are consistent with these findings. In contrast to our finding that α_2M^* induces Ca^{2+} oscillations in MSMCs, others have reported that α_2M^* caused stable $[Ca^{2+}]_i$ increases in macrophages (38), neurons (30), and trabecular meshwork cells (43). The mechanisms by which α_2M^* causes Ca^{2+} influx appear to be cell type-specific. In neurons, the increases in $[Ca^{2+}]_i$ result from activation of the NMDA receptor (30), an unlikely candidate in MSMCs in which Ca^{2+} predominantly enters by voltage-gated Ca^{2+} channels (44, 45), with contributions from receptor-operated Ca^{2+} channels and SOCs (6, 46). In macrophages, Misra et al. (47) proposed that GRP78, a 78-kDa glucose-regulated protein, is an alternative α_2M receptor. In the absence of GRP78, α_2M^* was unable to regulate IP_3 and cytosolic free Ca^{2+}. GRP78 increases in human myometrium in response to inflammation (48), is associated with the BK_{Ca} channel in mouse cochlea (49), and is elevated in labor or preterm labor compared with nonlabor myometrium (48). We cannot rule out the possibility that GRP78 serves as a receptor for α_2M^*. Nonetheless, our data showed that Ca^{2+} influx was inhibited in the presence of RAP, suggesting that LRP1 is the responsible receptor in hMSMCs. Although the identities of the SOCE proteins responsible for α_2M^*-regulated Ca^{2+} entry are unknown, evidence from other studies in MSMCs indicate that TRPC (50), STIM, and Orai (51) may contribute to this current. The SOCE blockers 2-APB and BTP2 both inhibit TRPC channels (52), suggesting that entry through TRPC was, in part, a component of the SOCE entry needed for the Ca^{2+} oscillations we observed in the MSMCs. Whether these channels are a functional component of the α_2M^*–LRP1–BK_{Ca} complex will be investigated in future studies.

We found that, in the absence of OXT, α_2M^* failed to produce Ca^{2+} oscillations, indicating that the cells must first be primed by Ca^{2+} release from the sarcoplasmic reticulum. Further studies will establish whether this stimulus is specific to OXT. Because OXT was present throughout the entire Ca^{2+} imaging time, it could be argued that OXT exerted a sustained effect on the cells. However, we did not observe an increase in $[Ca^{2+}]_i$ upon a second exposure to OXT, and previous studies have shown that 100 nM OXT desensitizes OXT receptors (39). Moreover, inactive α_2M did not induce Ca^{2+} oscillations after OXT application. Alternatively, α_2M^* might prevent OXT receptor downregulation through its antiprotease activity. However, we only observed oscillations in the presence of α_2M^*, which is in a locked conformation that cannot bind and clear proteases, thus excluding this possibility (53). We predict that in hMSMCs, a complex consisting of the OXT receptor, α_2M^*, LRP1, and BK_{Ca} synergistically regulates Ca^{2+} dynamics, which, in turn, control excitation-contraction coupling. In support of this idea, previous studies have indicated that LRP1 (54) and the BK_{Ca} channel (32) can localize to specialized lipid-rich membrane domains that facilitate signaling events by positioning functionally interacting molecules in close proximity (55, 56). Given the physical association between BK_{Ca}, α_2M^*, and LRP1, endocytosis mediated by α_2M^*-LRP1 (57, 58) may result in internalization of BK_{Ca} to decrease membrane localization and may represent another mode of α_2M^* action in MSMCs. This periodic removal of BK_{Ca} from the plasma membrane would provide an excitatory signal to elicit activation of SOCs and Ca^{2+} oscillations. Internalization of BK_{Ca} was recently demonstrated in arterial smooth muscle cells; in this case, angiotensin II signaling through PKC stimulated BK_{Ca} channel internalization (59). Likewise, in cardiomyocytes, ATP-sensitive K^+ channels are internalized to the endosome, where they serve as a reserve to be trafficked to the surface after cardiac ischemia (60). Thus, in MSMCs, internalization may provide a mechanism for rapid control of BK_{Ca} channel surface localization to control excitability at the critical juncture between nonlaboring and laboring states.

Data from this and other studies (61) indicate that α_2M is present in the myometrium; however, we detected the inactive α_2M form only in native tissue. This could be due to rapid degradation of α_2M^* by the endocytic machinery or destabilization of α_2M^* during sample preparation. Furthermore, we envision that α_2M^* secreted from other tissues, such as the decidua and placenta (24, 62), might contribute to the response in vivo. Our study indicates that, in addition to its roles in immune cell activation and migration (24), α_2M^* may affect pregnancy outcomes via cross-talk with the BK_{Ca} channel. We performed our experiments on isolated hMSMCs, but, in vivo, gap junction-mediated connectivity and enhanced intercellular communication of the hMSMCs at the end of pregnancy (63) could magnify α_2M^* action to promote uterine contraction. Both α_2M^* and the BK_{Ca} channel are conserved across species, and α_2M^* is the major endoprotease inhibitor in mammalian blood. However, whether α_2M^* and BK_{Ca} functionally interact in the myometrium of other mammals was not investigated.

In human parturition, an inflammatory process drives cervical ripening and myometrial activation (64), but the process by which inflammation leads to changes in excitability of MSMCs is unclear. Proinflammatory cytokines, such as TNF-α, TGF-β, and IL-1β, have been implicated to be triggers of both term and preterm labor (65–67) and can bind to and activate α_2M (24). Thus, we speculate that the proinflammatory state at the time of labor causes α_2M activation and binding to LRP1, endocytosis of this complex, and an increase in $[Ca^{2+}]_i$, thereby promoting uterine contractility. Moreover, IL-1β, a cytokine important in both term and preterm labor, enhances both basal entry and SOCE, but does not affect L- or T-type voltage-gated Ca^{2+} channels (25). Although the IL-1β–induced increase in $[Ca^{2+}]_i$ is likely due, in part, to the IL-1β receptor, additional signaling through the α_2M^* pathway may provide a mechanism for signal enhancement. Inflammation elicited by intrauterine infections can also promote abnormal and premature contractions of the myometrium and preterm labor (68), but whether α_2M^* is responsible for the uterine transition from quiescence to contractility is unclear. Further study to identify and dissect proteins and pathways that regulate ion channel activity to control uterine activity will continue to provide insights into the normal course of pregnancy.

ACKNOWLEDGMENTS. We thank Dr. Deborah J. Frank and Dr. Rachel Tribe for critical reading and editing of the manuscript, the Center for Investigation of Membrane Excitability Diseases at Washington University for Ca^{2+} imaging assistance, and the clinical research nurses for obtaining tissues. This work was supported by NIH Grant 5R01HD037831 (to S.K.E.).

1. Riemer RK, Heymann MA (1998) Regulation of uterine smooth muscle function during gestation. *Pediatr Res* 44(5):615–627.
2. Wray S, et al. (2003) Calcium signaling and uterine contractility. *J Soc Gynecol Investig* 10(5):252–264.
3. Marshall JM (1990) Relation between membrane potential and spontaneous contraction of the uterus. *Uterine Contractility. Mechanisms of Control*, ed Garfield RE (Sereno Symposia USA, Norwell, MA), pp 3–7.
4. Parkington HC, Coleman HA (1990) The role of membrane potential in the control of uterine motility. *Uterine Function: Molecular and Cellular Aspects*, eds Carston ME, Miller JD (Plenum, New York), pp 195–248.
5. Szal SE, et al. (1994) [Ca2+]i signaling in pregnant human myometrium. *Am J Physiol* 267(1 Pt 1):E77–E87.
6. Tribe RM, Moriarty P, Poston L (2000) Calcium homeostatic pathways change with gestation in human myometrium. *Biol Reprod* 63(3):748–755.

7. Aguilar HN, Mitchell BF (2010) Physiological pathways and molecular mechanisms regulating uterine contractility. *Hum Reprod Update* 16(6):725–744.
8. Haeberle JR, Hathaway DR, DePaoli-Roach AA (1985) Dephosphorylation of myosin by the catalytic subunit of a type-2 phosphatase produces relaxation of chemically skinned uterine smooth muscle. *J Biol Chem* 260(18):9965–9968.
9. Khan RN, Smith SK, Morrison JJ, Ashford ML (1997) Ca2+ dependence and pharmacology of large-conductance K+ channels in nonlabor and labor human uterine myocytes. *Am J Physiol* 273(5 Pt 1):C1721–C1731.
10. Chan YW, van den Berg HA, Moore JD, Quenby S, Blanks AM (2014) Assessment of myometrial transcriptome changes associated with spontaneous human labour by high-throughput RNA-seq. *Exp Physiol* 99(3):510–524.
11. Pérez GJ, Toro L, Erulkar SD, Stefani E (1993) Characterization of large-conductance, calcium-activated potassium channels from human myometrium. *Am J Obstet Gynecol* 168(2):652–660.
12. Tritthart HA, Mahnert W, Fleischhacker A, Adelwöhrer N (1991) Potassium channels and modulating factors of channel functions in the human myometrium. *Z Kardiol* 80(Suppl 7):29–33.
13. Anwer K, et al. (1993) Calcium-activated K+ channels as modulators of human myometrial contractile activity. *Am J Physiol* 265(4 Pt 1):C976–C985.
14. Nelson MT, et al. (1995) Relaxation of arterial smooth muscle by calcium sparks. *Science* 270(5236):633–637.
15. Burdyga T, Wray S, Noble K (2007) In situ calcium signaling: No calcium sparks detected in rat myometrium. *Ann N Y Acad Sci* 1101:85–96.
16. Moynihan AT, Smith TJ, Morrison JJ (2008) The relaxant effect of nifedipine in human uterine smooth muscle and the BK(Ca) channel. *Am J Obstet Gynecol* 198(2): 237–e231–e238.
17. Gao L, Cong B, Zhang L, Ni X (2009) Expression of the calcium-activated potassium channel in upper and lower segment human myometrium during pregnancy and parturition. *Reprod Biol Endocrinol* 7:27.
18. Matharoo-Ball B, Ashford ML, Arulkumaran S, Khan RN (2003) Down-regulation of the alpha- and beta-subunits of the calcium-activated potassium channel in human myometrium with parturition. *Biol Reprod* 68(6):2135–2141.
19. Hou S, Heinemann SH, Hoshi T (2009) Modulation of BKCa channel gating by endogenous signaling molecules. *Physiology (Bethesda)* 24:26–35.
20. Lu R, et al. (2006) MaxiK channel partners: Physiological impact. *J Physiol* 570(Pt 1): 65–72.
21. Singh H, et al. (2013) MitoBK(Ca) is encoded by the Kcnma1 gene, and a splicing sequence defines its mitochondrial location. *Proc Natl Acad Sci USA* 110(26): 10836–10841.
22. Singh H, Stefani E, Toro L (2012) Intracellular BK(Ca) (iBK(Ca)) channels. *J Physiol* 590(23):5937–5947.
23. Toro L, et al. (2014) MaxiK channel and cell signalling. *Pflugers Arch* 466(5):875–886.
24. Tayade C, Esadeg S, Fang Y, Croy BA (2005) Functions of alpha 2 macroglobulins in pregnancy. *Mol Cell Endocrinol* 245(1-2):60–66.
25. Tribe RM, Moriarty P, Dalrymple A, Hassoni AA, Poston L (2003) Interleukin-1beta induces calcium transients and enhances basal and store operated calcium entry in human myometrial smooth muscle. *Biol Reprod* 68(5):1842–1849.
26. Sayegh RA, Tao XJ, Leykin L, Isaacson KB (1997) Endometrial alpha-2 macroglobulin; localization by in situ hybridization and effect on mouse embryo development in vitro. *J Clin Endocrinol Metab* 82(12):4189–4195.
27. Rehman AA, Ahsan H, Khan FH (2013) α-2-Macroglobulin: A physiological guardian. *J Cell Physiol* 228(8):1665–1675.
28. Borth W (1992) Alpha 2-macroglobulin, a multifunctional binding protein with targeting characteristics. *FASEB J* 6(15):3345–3353.
29. LaMarre J, Wollenberg GK, Gonias SL, Hayes MA (1991) Cytokine binding and clearance properties of proteinase-activated alpha 2-macroglobulins. *Lab Invest* 65(1): 3–14.
30. Bacskai BJ, Xia MQ, Strickland DK, Rebeck GW, Hyman BT (2000) The endocytic receptor protein LRP also mediates neuronal calcium signaling via N-methyl-D-aspartate receptors. *Proc Natl Acad Sci USA* 97(21):11551–11556.
31. Li Y, Lorca RA, Ma X, Rhodes A, England SK (2014) BK channels regulate myometrial contraction by modulating nuclear translocation of NF-κB. *Endocrinology* 155(8): 3112–3122.
32. Brainard AM, Miller AJ, Martens JR, England SK (2005) Maxi-K channels localize to caveolae in human myometrium: A role for an actin-channel-caveolin complex in the regulation of myometrial smooth muscle K+ current. *Am J Physiol Cell Physiol* 289(1): C49–C57.
33. Grynkiewicz G, Poenie M, Tsien RY (1985) A new generation of Ca2+ indicators with greatly improved fluorescence properties. *J Biol Chem* 260(6):3440–3450.
34. Kim EY, Ridgway LD, Dryer SE (2007) Interactions with filamin A stimulate surface expression of large-conductance Ca2+-activated K+ channels in the absence of direct actin binding. *Mol Pharmacol* 72(3):622–630.
35. Shmygol A, Noble K, Wray S (2007) Depletion of membrane cholesterol eliminates the Ca2+-activated component of outward potassium current and decreases membrane capacitance in rat uterine myocytes. *J Physiol* 581(Pt 2):445–456.
36. Söderberg O, et al. (2006) Direct observation of individual endogenous protein complexes in situ by proximity ligation. *Nat Methods* 3(12):995–1000.
37. Dixon SJ, Aubin JE (1987) Serum and alpha 2-macroglobulin induce transient hyperpolarizations in the membrane potential of an osteoblastlike clone. *J Cell Physiol* 132(2):215–225.
38. Misra UK, Chu CT, Rubenstein DS, Gawdi G, Pizzo SV (1993) Receptor-recognized alpha 2-macroglobulin-methylamine elevates intracellular calcium, inositol phosphates and cyclic AMP in murine peritoneal macrophages. *Biochem J* 290(Pt 3):885–891.
39. Willets JM, et al. (2009) Regulation of oxytocin receptor responsiveness by G protein-coupled receptor kinase 6 in human myometrial smooth muscle. *Mol Endocrinol* 23(8):1272–1280.
40. Hawkins JS, Wing DA (2012) Current pharmacotherapy options for labor induction. *Expert Opin Pharmacother* 13(14):2005–2014.
41. Gravina FS, et al. (2010) Role of mitochondria in contraction and pacemaking in the mouse uterus. *Br J Pharmacol* 161(6):1375–1390.
42. Li B, et al. (2014) Nuclear BK channels regulate gene expression via the control of nuclear calcium signaling. *Nat Neurosci* 17(8):1055–1063.
43. Howard GC, Roberts BC, Epstein DL, Pizzo SV (1996) Characterization of alpha 2-macroglobulin binding to human trabecular meshwork cells: Presence of the alpha 2-macroglobulin signaling receptor. *Arch Biochem Biophys* 333(1):19–26.
44. Blanks AM, et al. (2007) Characterization of the molecular and electrophysiological properties of the T-type calcium channel in human myometrium. *J Physiol* 581(Pt 3): 915–926.
45. Young RC, Smith LH, McLaren MD (1993) T-type and L-type calcium currents in freshly dispersed human uterine smooth muscle cells. *Am J Obstet Gynecol* 169(4):785–792.
46. Putney JW, Jr (1986) A model for receptor-regulated calcium entry. *Cell Calcium* 7(1): 1–12.
47. Misra UK, Gonzalez-Gronow M, Gawdi G, Wang F, Pizzo SV (2004) A novel receptor function for the heat shock protein Grp78: Silencing of Grp78 gene expression attenuates alpha2M*-induced signalling. *Cell Signal* 16(8):929–938.
48. Liong S, Lappas M (2014) Endoplasmic reticulum stress is increased after spontaneous labor in human fetal membranes and myometrium where it regulates the expression of prolabor mediators. *Biol Reprod* 91(3):70.
49. Kathiresan T, Harvey M, Orchard S, Sakai Y, Sokolowski B (2009) A protein interaction network for the large conductance Ca(2+)-activated K(+) channel in the mouse cochlea. *Mol Cell Proteomics* 8(8):1972–1987.
50. Dalrymple A, Slater DM, Beech D, Poston L, Tribe RM (2002) Molecular identification and localization of Trp homologues, putative calcium channels, in pregnant human uterus. *Mol Hum Reprod* 8(10):946–951.
51. Chin-Smith EC, Slater DM, Johnson MR, Tribe RM (2014) STIM and Orai isoform expression in pregnant human myometrium: A potential role in calcium signaling during pregnancy. *Front Physiol* 5:169.
52. He LP, Hewavitharana T, Soboloff J, Spassova MA, Gill DL (2005) A functional link between store-operated and TRPC channels revealed by the 3,5-bis(trifluoromethyl)pyrazole derivative, BTP2. *J Biol Chem* 280(12):10997–11006.
53. Sottrup-Jensen L, Petersen TE, Magnusson S (1981) Mechanism of proteinase complex formation with alpha 2-macroglobulin. Three modes of trypsin binding. *FEBS Lett* 128(1):127–132.
54. Zhang H, et al. (2004) Localization of low density lipoprotein receptor-related protein 1 to caveolae in 3T3-L1 adipocytes in response to insulin treatment. *J Biol Chem* 279(3):2221–2230.
55. Galbiati F, Razani B, Lisanti MP (2001) Emerging themes in lipid rafts and caveolae. *Cell* 106(4):403–411.
56. Isshiki M, Anderson RG (2003) Function of caveolae in Ca2+ entry and Ca2+-dependent signal transduction. *Traffic* 4(11):717–723.
57. Herz J, Strickland DK (2001) LRP: A multifunctional scavenger and signaling receptor. *J Clin Invest* 108(6):779–784.
58. Higuchi M, et al. (1994) Expression of the alpha 2-macroglobulin-encoding gene in rat brain and cultured astrocytes. *Gene* 141(2):155–162.
59. Leo MD, et al. (2015) Angiotensin II stimulates internalization and degradation of arterial myocyte plasma membrane BK channels to induce vasoconstriction. *Am J Physiol Cell Physiol* 309(6):C392–C402.
60. Bao L, Hadjiolova K, Coetzee WA, Rindler MJ (2011) Endosomal KATP channels as a reservoir after myocardial ischemia: A role for SUR2 subunits. *Am J Physiol Heart Circ Physiol* 300(1):H262–H270.
61. Huang C, Jeffrey JJ (1998) Serotonin regulates the expression of the gene for alpha2-macroglobulin in myometrial smooth muscle cells. *Mol Cell Endocrinol* 139(1-2):79–87.
62. Siu SS, Choy MY, Leung TN, Lau TK (2006) Lack of site-specific production of decidual alpha-2 macroglobulin in human pregnancy. *J Soc Gynecol Investig* 13(7):491–496.
63. Miyoshi H, Boyle MB, MacKay LB, Garfield RE (1998) Gap junction currents in cultured muscle cells from human myometrium. *Am J Obstet Gynecol* 178(3):588–593.
64. Bisits AM, et al. (2005) Inflammatory aetiology of human myometrial activation tested using directed graphs. *PLOS Comput Biol* 1(2):132–136.
65. Bowen JM, Chamley L, Mitchell MD, Keelan JA (2002) Cytokines of the placenta and extra-placental membranes: Biosynthesis, secretion and roles in establishment of pregnancy in women. *Placenta* 23(4):239–256.
66. Kelly RW (1996) Inflammatory mediators and parturition. *Rev Reprod* 1(2):89–96.
67. Romero R, Erez O, Espinoza J (2005) Intrauterine infection, preterm labor, and cytokines. *J Soc Gynecol Investig* 12(7):463–465.
68. Goldenberg RL, Hauth JC, Andrews WW (2000) Intrauterine infection and preterm delivery. *N Engl J Med* 342(20):1500–1507.
69. Bustin SA, et al. (2009) The MIQE guidelines: Minimum information for publication of quantitative real-time PCR experiments. *Clin Chem* 55(4):611–622.